International Journal of Applied Engineering Research ISSN 0973-4562 Volume 14, Number 1 (2019) pp. 284-295

Unsteady MHD Convective flow of Rivlin-Ericksen Fluid over an Infinite Vertical Porous Plate with Absorption Effect and Variable Suction

B.Veera Sankar[1*] and B.Rama Bhupal Reddy[2]

[1]Research Scholar, Department of Mathematics, Rayalaseema University, Kurnool, Andhra Pradesh-518007, India (*- Corresponding author)*

[2]Professor and Head, Department of Mathematics, KSRM College of Engineering, Kadapa, Andhra Pradesh-516003, India

Abstract

We have considered the boundary-layer flow of a heat-absorbing MHD Rivlin–Ericksen fluid along a semi-infinite vertical permeable moving plate in the presence of thermal buoyancy effect. The dimensionless governing equations are solved analytically using two-term harmonic and non-harmonic functions. Quantitative analysis of the results is presented with a view to disclose for the velocity and temperature profiles within the boundary layer. The Skin friction and Nusselt number are also examined with the reference to governing parameters.

Keywords: MHD flows, Rivlin–Ericksen flow, porous medium and unsteady flows

NOMENCLATURE:

u, v	Components of velocities along the *x* and *z* directions respectively
x, z	Distances along and perpendicular to the plate, respectively
V_0	Scale of suction velocity
A	suction velocity parameter
B_0	magnetic induction
C_p	specific heat at constant pressure
Gr	Grashof number
g	acceleration due to gravity
k_1	permeability of the porous medium
K	permeability parameter
M	magnetic field parameter
N	dimensionless material parameter
Pr	Prandtl number
n	dimensionless exponential index
Q_0	heat absorption coefficient
Nu	Nusselt number
T	temperature
t	dimensionless time
U_0	scale of free steam velocity
Q	Dimensionless viscoelasticity parameter of the Rivlin-Ericksen fluid
Rm	constant plate moving velocity

Greek symbol

α	fluid thermal diffusivity
β_T	coefficient of volumetric expansion of the working fluid
β_1	kinematic viscoelasticity
ε	scalar constant
k	thermal conductivity
τ	skin-friction coefficient
z	dimensionless normal distance
σ	electrical conductivity
ρ	fluid dencity
μ	fluid dynamic viscocity
ν	fluid kinematic viscocity
τ	Friction coefficient
θ	Dimensionless temperature

Superscripts

$'$	Differentiation with respect to z
*	Dimensional properties

Subscripts

p	plate
w	wall condition
∞	free steam condition

1. INTRODUCTION

MHD flows through porous media has been a subject of great interest for the last few decades. This was numerous thermal engineering applications in various disciplines, such as geophysical, thermal and insulation engineering, the modeling of packed sphere beds, the cooling of electronic systems, chemical catalytic reactors, ceramic processes, grain storage devices fiber and granular insulation, petroleum reservoirs, coal combustors, ground water pollution and filtration processes. Manu authors [1-12] investigated an unsteady MHD convective heat transfer past a semi-infinite vertical porous plate. Seethamahalakshmi et al. [13] discussed MHD free convective mass transfer flow past an infinite vertical porous plate with variable suction and soret effect. Rajesh *et al.* [14] studied radiation and mass transfer effects on MHD free convection flow past an exponentially accelerated vertical plate with variable temperature. Israel-Cookey et al. [15] studied the influence of viscous dissipation on unsteady MHD free convection flow past an infinite heated vertical plate in porous medium with time-dependent suction. Raju *et al.* [16] studied unsteady MHD free convective oscillatory couette flow through a porous medium with periodic wall temperature.

The Rivlin–Ericksen elastic-viscous fluid has relevance and importance in geophysical fluid dynamics, chemical technology and industry. Some authors [17-34] discussed in this area considering Rivlin–Ericksen viscoelastic fluid in a porous medium. Recently, Krishna et al [35-38] discussed the MHD flows of an incompressible and electrically conducting fluid in planar channel. Veera Krishna et al. [39] discussed heat and mass transfer on unsteady MHD oscillatory flow of blood through porous arteriole. The effects of radiation and Hall current on an unsteady MHD free convective flow in a vertical channel filled with a porous medium have been studied by Veera Krishna et al. [40]. The heat generation/absorption and thermo-diffusion on an unsteady free convective MHD flow of radiating and chemically reactive second grade fluid near an infinite vertical plate through a porous medium and taking the Hall current into account have been studied by Veera Krishna and Chamkha [41].

Motivated by the above studies, in this paper we have considered Rivlin–Ericksen fluid past a semi-infinite moving porous plate.

2. FORMULATION AND SOLUTION OF THE PROBLEM

We consider the MHD flow of an electrically conducting and heat absorbing Rivlin-Ericksen fluid over a semi-infinite vertical permeable moving plate embedded in a porous medium with a uniform transverse magnetic field (Fig.1). It is assumed that there is no applied voltage which implies the absence of a electrical field the transversely applied magnetic field and magnetic Reynolds number are assumed to be very small to that the induced magnetic field and the hall effects are negligible. A consequence of the small magnetic Reynolds number is a the uncoupling of the Navier-stokes equations from Maxwell's equations the governing equations for this investigation are based on the balances of mass, linear momentum made above, these equations can be written in Cartisian frame of reference as follows:

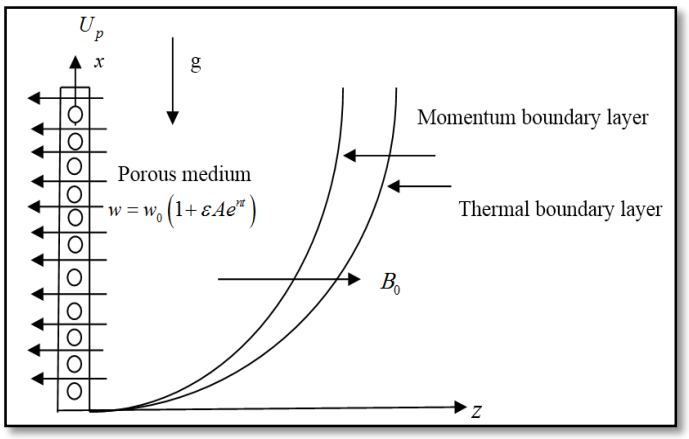

Fig. 1 Physical configuration of the Problem

$$\frac{\partial w}{\partial z} = 0 \tag{1}$$

$$\frac{\partial u}{\partial t} + w\frac{\partial u}{\partial z} = -\frac{1}{\rho}\frac{\partial p}{\partial x} + \frac{\partial^2 u}{\partial z^2} - \beta_1\left(\frac{\partial^3 u}{\partial t \partial z^2} + v\frac{\partial^3 u}{\partial z^3}\right) - \frac{\sigma B_0^2}{\rho}u - \frac{v}{k_1}u + \beta_T\left(T - T_\infty\right) \tag{2}$$

$$\frac{\partial v}{\partial t} + w\frac{\partial v}{\partial z} = -\frac{1}{\rho}\frac{\partial \rho}{\partial y} + v\frac{\partial^2 v}{\partial z^2} - \beta_1\left(\frac{\partial^3 v}{\partial z^2 \partial t} + \frac{\partial^3 v}{\partial z^3}\right) - \frac{\sigma B_0^2}{\rho}v - \frac{v}{k_1}v \tag{3}$$

$$\frac{\partial T}{\partial t} + w\frac{\partial T}{\partial z} = \alpha\frac{\partial^2 T}{\partial z^2} - \frac{Q_0}{\rho C_p}\left(T - T_\infty\right) \tag{4}$$

The magnetic and viscous dissipations are neglected in this study. It is assumed that the permeable plate moves with a constant velocity in the direction of fluid flow and the free steam velocity follows the exponentially increasing small perturbation law. In addition, it is assumed that the tempareture at the wall as well as the suction velocity is exponentially varying with time. Under then assumptions the appropriate conditions for the velocity, temperature fields are

$$u = U_p,\ v = 0,\ T = T_w + \varepsilon\left(T_w - T_\infty\right)e^{nt} \quad \text{at} \quad z = 0, \tag{5}$$

$$u \to U_\infty, v \to 0 = u_0\left(1+\varepsilon e^{nt}\right), T \to T_\infty, \quad \text{as} \quad z \to \infty \tag{6}$$

Where, U_p, T_w are the wall dimensional velocity temperature, respectively U_∞, T_∞ are the free steam dimensional velocity, temperature respectively, u_0 and η are constants.

It is clear from equation (1) that the suction velocity at the plate surface is a function of time only assuming that it takes the following exponential form

$$w = -w_0\left(1+\varepsilon A e^{nt}\right) \tag{7}$$

Combining equations (2) and (3), let
$q = u + iv$ and $\xi = x - iy$, we obtain,

$$\frac{\partial q}{\partial t} + w\frac{\partial q}{\partial z} = -\frac{1}{\rho}\frac{\partial p}{\partial \xi} + \nu\frac{\partial^2 q}{\partial z^2} - \beta_1\left(\frac{\partial^3 q}{\partial z^2 \partial t} + \nu\frac{\partial^3 q}{\partial z^3}\right) - \left(\frac{\sigma B_0^{\,2}}{\rho} + \frac{\nu}{k_1}\right)q + g\beta_T\left(T - T_\infty\right) \tag{8}$$

Where A is a real positive constants, ε and εA are small less then unity, and w_0 is a scale of suction velocity which has non-zero posstive constant outside the boundary layer equation (2) gives

$$-\frac{1}{\rho}\frac{\partial p}{\partial \xi} = \frac{\partial U_\infty}{\partial t} + \frac{\nu}{k}U_\infty + \frac{\sigma}{\rho}B_0^2 U_\infty \tag{9}$$

We introduced the following non-dimensional variables

$$u^* = \frac{u}{U_0}, v^* = \frac{v}{w_0}, z^* = \frac{w_0 z}{\nu}, U_\infty^* = \frac{U_\infty}{U_0},$$
$$U_p^* = \frac{u_p}{U_0}, t^1 = \frac{t w_0^2}{\nu}, \theta = \frac{\mathrm{T} - \mathrm{T}_\infty}{\mathrm{T}_w - \mathrm{T}_\infty}$$

Making use of non-dimensional variables the governing equations reduces to (Droppingaskerisks)

$$\frac{\partial q}{\partial t} - \left(1+\varepsilon A e^{nt}\right)\frac{\partial q}{\partial z} = \frac{\partial U_\infty}{\partial t} + \frac{\partial^2 q}{\partial z^2} + \mathrm{Gr}\,\theta + N\left(U_\infty - q\right) - Rm\frac{\partial^3 u}{\partial t \partial z^2} - \left(1+\varepsilon A e^{nt}\right)\frac{\partial^3 q}{\partial z^3} \tag{10}$$

$$\frac{\partial \theta}{\partial t} - \left(1+\varepsilon A e^{nt}\right)\frac{\partial \theta}{\partial z} = \frac{1}{\mathrm{Pr}}\frac{\partial^2 \theta}{\partial z^2} - Q\theta \tag{11}$$

Where, $K = \frac{k_1 w_0}{\nu^2}$ is the permeability parameter, $\mathrm{Pr} = \frac{\nu\rho C_p}{k}$ is the prandtl number, $M^2 = \frac{\sigma B_0^2 \nu}{\rho w_0^2}$ is the magnetic field parameter, $\mathrm{Gr} = \frac{\nu\beta_T g\left(T_\infty - T_\infty\right)}{w_0^3}$ is the Grashof number, $Rm = \frac{\beta_1 w_0^2}{\nu^2}$ is the dimensionless form visco-elasticity parameter of the Rivlin-Ericksen Fluid.

The dimensionless form the boundary conditions equations (5) and (6) become

$$\begin{aligned} &q = U_p, \theta = 1+\varepsilon e^{nt}, U = 1+\varepsilon e^{nt} && \text{at} \quad z = 0 \\ &q \to U_\infty, \theta = 0, U \to 0 && \text{at} \quad z \to \infty \end{aligned} \tag{12}$$

Equation (10) and (11) represent a set of partial differential equations that cannot be solved in closed form however if can be reduced to a set off ordinary differential equations in dimensionless fom that can be solved analytically this can be done representing the velocity and temperature as,

$$q = q_0\left(z\right) + \varepsilon e^{nt} q_1\left(z\right) + O\left(\varepsilon^2\right) \tag{13}$$

$$\theta = \theta_0\left(z\right) + \varepsilon e^{nt}\theta_1\left(z\right) + O\left(\varepsilon^2\right) \tag{14}$$

Substituting the equations (13) and (14) into equation (10) and(11),equating the harmonic and non-hamonic terms, the neglecting and higher order terms of $O\left(\varepsilon^2\right)$,one obtains the following pairs of equations $\left(q_0, \theta_0\right)$ and $\left(q_1, \theta_1\right)$,

$$Rm\frac{d^3 q_0}{dz^3} + \frac{d^2 q_0}{dz^2} + \frac{dq_0}{dz} - Nq_0 = -\mathrm{Gr}\,\theta_0 - N \tag{15}$$

$$Rm\frac{d^3 q_1}{dz^3} + \left(1 - nRm\right)\frac{d^2 q_1}{dz^2} + \frac{dq_1}{dz} - Nq_1 - nq_1 = -n - Gr\theta_1 - N - RmA\frac{d^3 q_0}{dz^3} - A\frac{dq_0}{dz} \tag{16}$$

$$\frac{d^2\theta_0}{d^2 z} + \mathrm{Pr}\frac{d\theta_0}{dz} - Q\mathrm{Pr}\,\theta_0 = 0 \tag{17}$$

$$\frac{d^2\theta_1}{dz^2} + \mathrm{Pr}\frac{d\theta_1}{dz} - n\mathrm{Pr}\,\theta_1 - Q\mathrm{Pr}\,\theta_1 = -A\mathrm{Pr}\frac{d\theta_0}{dz} \tag{18}$$

The corresponding boundary conditions can be written as

$$\begin{aligned} &q_0 = U_p, q_1 = 0, \theta_0 = 1, \theta_1 = 1 && \text{at} \quad z = 0 \\ &q_0 = 1,\ q_1 = 1,\ \theta_0 \to 0,\ q_1 \to 0 && \text{at} \quad z \to \infty \end{aligned} \tag{19}$$

Without going into detail,the solution of equation (15)-(18) subject to conditions (19) can be show to be

$$q_0 = e^{-m_1 z} \tag{20}$$

$$q_1 = a_2 e^{-m_3 z} + a_1 e^{-m_1 z} \tag{21}$$

Equations (15) an (16) are third degree order differential equations when $Rm \neq 0$ and we have two boundary conditions so we follows bears and Walter's as

$$q_0 = q_{01} + Rmq_{02} + O\left(Rm^2\right) \tag{22}$$

$$q_1 = q_{11} + Rmq_{12} + O\left(Rm^2\right) \tag{23}$$

Substituting equations (22) and (20) into (15) and (16), equiating different powers of *Rm* and neglecting $O\left(Rm^2\right)$ are,

$$\frac{d^2q_{01}}{dz^2} + \frac{dq_{01}}{dz} - Nq_{01} = -\mathrm{Gr}e^{-m_1 z} - N \tag{24}$$

$$\frac{d^3q_{01}}{\partial z^3} + \frac{d^2q_{02}}{dz^2} + \frac{dq_{02}}{dz} - Nq_{02} = 0 \tag{25}$$

$$\begin{aligned}\frac{d^2q_{11}}{dz^2} + \frac{dq_{11}}{dz} - \left(n+N\right)q_{11} \\ = -n - \mathrm{Gr}\left(a_1e^{-m_1 z} + a_2e^{-m_3 z}\right) - N - A\frac{dq_{01}}{dz}\end{aligned} \tag{26}$$

$$\begin{aligned}\frac{d^3q_{11}}{dz^3} + \frac{d^2q_{12}}{dz^2} - n\frac{d^2q_{11}}{dz^2} + \frac{dq_{12}}{dz} \\ -\left(n+N\right)q_{12} = -A\frac{d^3q_{01}}{dz^3} - A\frac{dq_{02}}{dz}\end{aligned} \tag{27}$$

The corresponding boundary conditions are

$$q_{01} = u_p, q_{02} = 0, q_{11} = 0, q_{12} = 0 \quad \text{at} \quad z = 0$$

$$q_{01} = 1, q_{02} = 0, q_{11} = 1, q_{12} = 0, \quad \text{as} \quad z \to \infty \tag{24}$$

We get zeroth order and first order solutions of Rm

$$q_{01} = a_4e^{-m_6 z} + a_3e^{-m_1 z} + 1 \tag{25}$$

$$q_{02} = a_7e^{-m_8 z} + a_5e^{-m_6 z} + a_6e^{-m_1 z} \tag{26}$$

$$q_{11} = -a_{16}e^{-m_{10} z} + a_{14} + a_9e^{-m_3 z} + a_{15}e^{-m_1 z} + a_{12}e^{-m_6 z} \tag{27}$$

$$\begin{aligned}q_{12} = -a_{27}e^{-m_{12} z} + a_{22}e^{-m_6 z} + a_{23}e^{-m_1 z} \\ + a_{24}e^{-m_8 z} + a_{25}e^{-m_{10} z} + a_{26}e^{-m_3 z}\end{aligned} \tag{28}$$

In view of the above solutions, the velocity and tempareture distributions in the boundary layer become

$$\begin{aligned}q\left(z,t\right) &= q_0\left(z\right) + \varepsilon e^{nt}q_1\left(z\right) \\ &= \left[\left(a_4e^{-m_6 z} + a_3e^{-m_1 z}\right) + Rm\left(a_7e^{-m_8 z} + a_5e^{-m_6 z} + a_6e^{-m_1 z}\right)\right] \\ &+ \varepsilon e^{nt}\left[\left(-a_{16}e^{-m_{10} z} + a_{14} + a_9e^{-m_3 z} + a_{15}e^{-m_1 z} + a_{12}e^{-m_6 z}\right)\right. \\ &\left. + Rm\left(-a_{27}e^{-m_{12} z} + a_{22}e^{-m_6 z} + a_{23}e^{-m_1 z} + a_{24}e^{-m_8 z} + a_{25}e^{-m_{10} z} + a_{26}e^{-m_3 z}\right)\right]\end{aligned}$$

$$\theta\left(z,t\right) = \theta_0\left(z\right) + \varepsilon e^{nt}\theta_1\left(z\right) \tag{29}$$

$$= e^{-m_1 z} + \varepsilon e^{nt}\left(a_2e^{-m_3 z} + a_1e^{-m_1 z}\right) \tag{30}$$

The skin friction co-efficient and Nusselt number are important physical parameters for this type of boundary-layer flow.These parameters can be defined and determined as follows.

$$\tau = \left(\frac{\partial q}{\partial z}\right)_{z=0} = \left(a_{28} + Rma_{29}\right) + \varepsilon e^{nt}\left(a_{30} + Rma_{31}\right) \tag{31}$$

$$Nu = \left(\frac{\partial \theta}{\partial z}\right)_{z=0} = a_{32} + \varepsilon e^{nt}\left(a_{33}\right) \tag{32}$$

3. RESULTS AND DISCUSSION

In order to get physical insight into the problem, the effects of various parameters encountered in the equations of the problem are analyzed on velocity and temperature fields with the help of figures (2-11). We have also analyzed the effects of these physical parameters on skin friction coefficient and Nusselt number and are mentioned in the tables (1-2). We noticed that, the velocity component *u* and *v* reduces with increasing the intensity of the magnetic field or Hartmann number *M.* The similar behaviour is observed for the resultant velocity (Figs. 2). It is obvious that the effect of increasing values of the magnetic field parameter M results in a decreasing velocity components *u* and *v* across the boundary layer. Figs. (3) depicts the effect of permeability of the porous medium parameter (*K*) on velocity distribution profiles for *u* and *v* and it is obvious that as permeability parameter (*K*) increases, the velocity components for *u* and *v* increases along the boundary layer thickness which is expected since when the holes of porous medium become larger, the resistive of the medium may be neglected. Similar behaviour is observed with increasing permeability parameter *K* for the resultant velocity. Figs. 5 illustrate the variation in velocity components *u* and *v* with span wise coordinate *n* for several values of Rm. We observed that both *u* reduces and *v* increases with increasing visco-elastic fluid parameter of the Rivlin-Ericksen fluid Rm. It was found that an increase in Rm leads to a decrease in the resultant velocity distribution across the boundary layer. Figs. (5) illustrate the velocity profiles for *u* and *v* for different values of the Grashof number Gr. It can be seen that an increase in Gr leads to a rise in velocity *u* and *v* profiles. The

resultant velocity is also enhances throughout the fluid region with increasing the thermal Grashof number Gr. We noticed that from the Figs. (6), the magnitude of the velocity component u reduces and v enhances with increasing Suction parameter A throughout the fluid region. The resultant velocity is reduces with increasing Suction parameter A. Figs. (7) presents the velocity distribution profiles for different values of the Prandtl number (Pr). The results show that the effect of increasing values of the prandtl number results in an increase in u and in a decrease in the velocity component v. The resultant velocity is also reduces with Prandtl number Pr. Figs. (8) shows the velocity profiles for u and v for different values of dimensionless heat absorption coefficient Q. Clearly as Q increase the pack values of velocity components u increase and v tends to decrease. The resultant velocity reduces with increasing heat absorption coefficient Q, physically the presence of heat absorption coefficient has the tendency to reduce the fluid temperature. This causes the thermal buoyancy effects to decrease resulting in a net reduction in the fluid velocity. The Figs. (9) shows the velocity profiles for u and v against span wise direction for different values of the scalar constant ε. It was found that an increase in the value of ε leads to an increase in the resultant velocity distribution across the boundary layer. The velocity component u diminishes first and then experiences enhancement and where as v increases with increasing the scalar constant ε. Finally, Figs. (10) depicts the effect of the frequency of oscillation n on the velocity distribution. The primary velocity component u and secondary velocity v reduce with increasing the frequency of oscillation n. The resultant velocity reduces with increasing the frequency of oscillation throughout the fluid medium.

We noticed that from the Figs. 11, the temperature reduces with increasing Prandtl number Pr or the frequency of oscillation n or suction velocity A or heat absorption coefficient Q. The result display that an increase in the value of Q results in decrease in the temperature profiles as expected. The temperature profiles with span wise coordinate n for various scalar constant ε. The numerical results show that the effect of increase value of e results in an increase thermal boundary layer thickness and more uniform temperature distribution across the boundary layer. Similar behaviour is observed in entire fluid region with increasing time.

We have also shown Table (1) of the surface skin friction coefficient against some parameters. The stress components τ_x and the magnitude of τ_y are reduces with increasing the intensity of the magnetic field M or the suction velocity A. The reversal behaviour is observed throughout the region with increasing Grashof number Gr or heat absorption coefficient Q or scalar constant ε, because an increase in Gr influences the buoyancy that results in skin friction. The stress component τ_x enhances and the magnitude of τ_y reduces with increasing permeability parameter K, where as τ_x decreases and the magnitude of τ_y boost up with increasing visco-elastic fluid parameter of the Rivlin-Ericksen fluid Rm or Prandtl number Pr or frequency of oscillation n.

The rate of heat transfer (Nu) is shown in the Table (2) with reference to all governing parameters. The magnitude of the Nusselt number rise up throughout the fluid region with increasing scalar constant ε, suction velocity A, Prandtl number Pr, heat absorption parameter Q and the frequency of oscillation n.

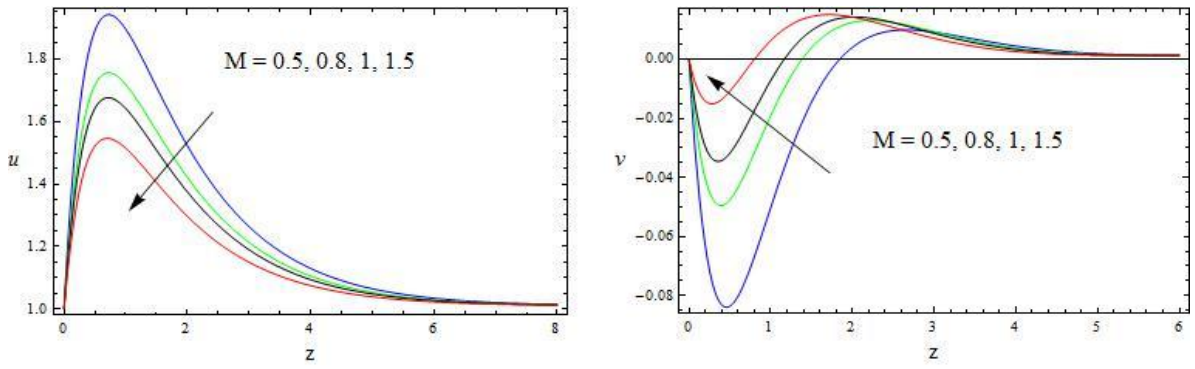

Figures 2. The velocity Profiles for u and v against M

$\varepsilon = 0.01, n = 0.5, A = 0.5, K = 0.5, \mathrm{Gr} = 3, Q = 0.1, \mathrm{Rm} = 0.01, \mathrm{Pr} = 0.71$

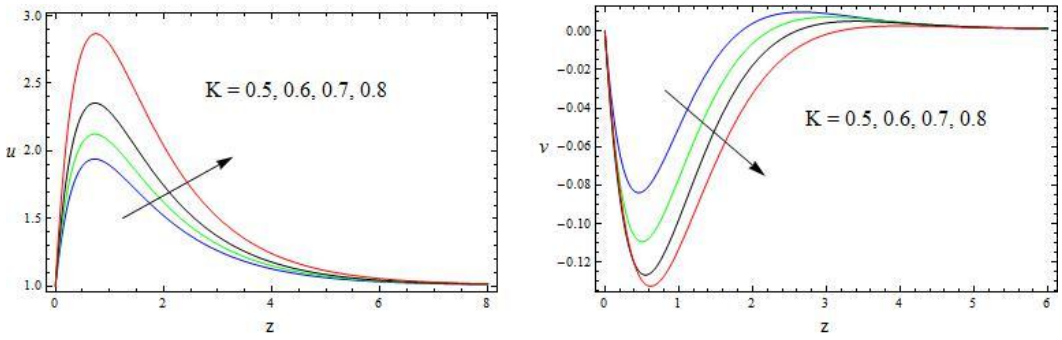

Figures 3. The velocity Profiles for u and v against K

$M = 0.5, \varepsilon = 0.01, n = 0.5, A = 0.5,\ \mathrm{Gr} = 3, Q = 0.1, \mathrm{Rm} = 0.01, \mathrm{Pr} = 0.71$

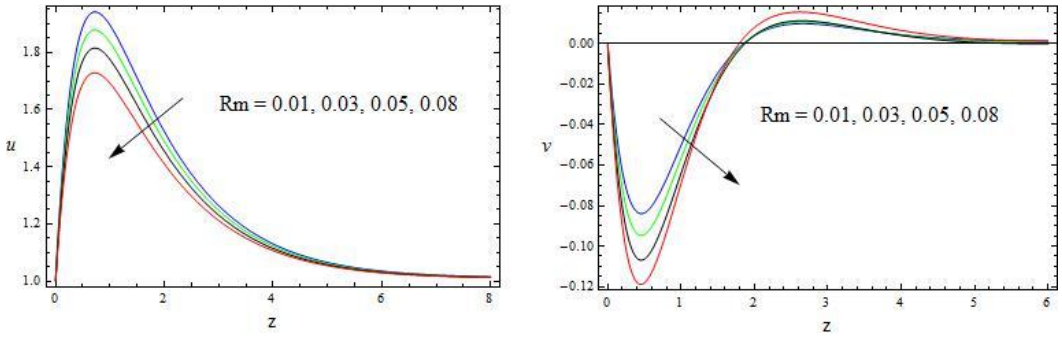

Figures 4. The velocity Profiles for u and v against R_m

$M = 0.5, \varepsilon = 0.01, n = 0.5, A = 0.5, K = 0.5, \mathrm{Gr} = 3, Q = 0.1, \mathrm{Pr} = 0.71$

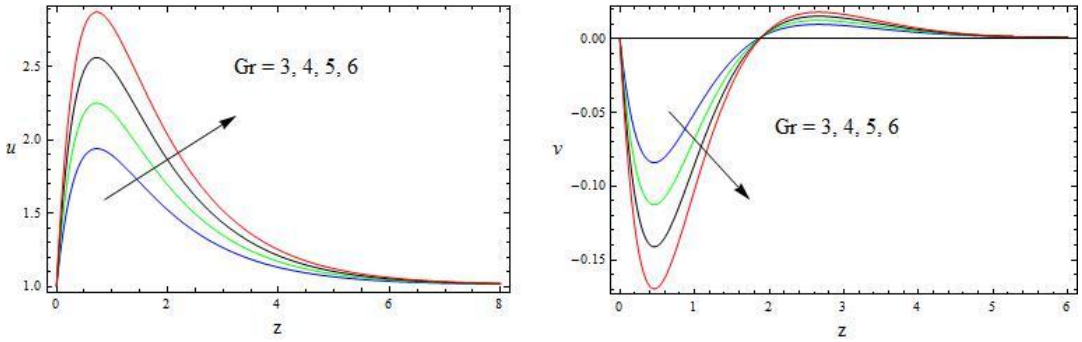

Figures 5. The velocity Profiles for u and v against Gr

$M = 0.5, \varepsilon = 0.01, n = 0.5, A = 0.5, K = 0.5, Q = 0.1, \mathrm{Rm} = 0.01, \mathrm{Pr} = 0.71$

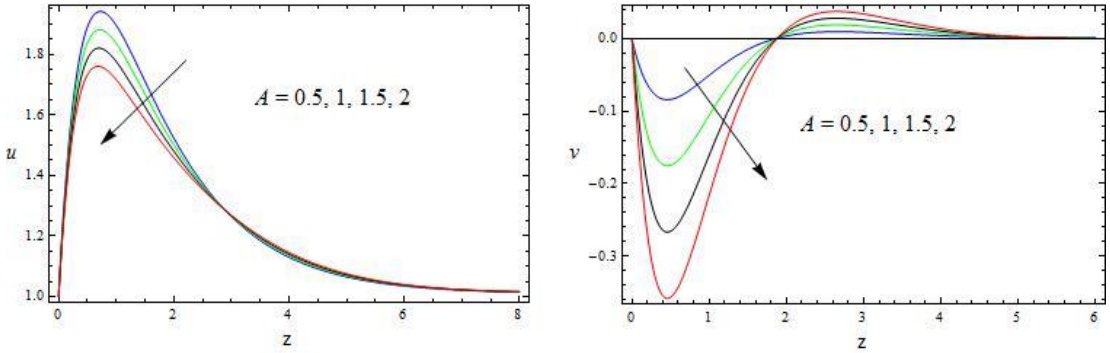

Figures 6. The velocity Profiles for u and v against A

$M = 0.5, \varepsilon = 0.01, n = 0.5,\ K = 0.5, \mathrm{Gr} = 3, Q = 0.1, \mathrm{Rm} = 0.01, \mathrm{Pr} = 0.71$

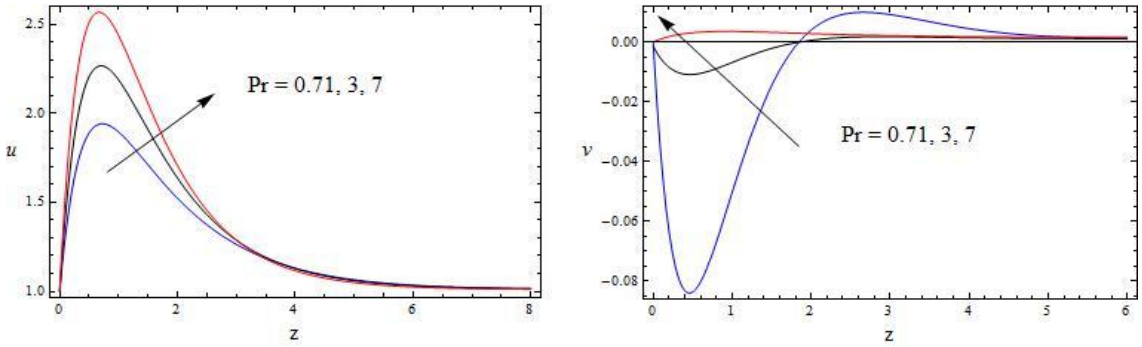

Figures 7. The velocity Profiles for u and v against Pr

$M = 0.5, \varepsilon = 0.01, A = 0.5, K = 0.5, n = 0.5, \mathrm{Gr} = 3, Q = 0.1, \mathrm{Rm} = 0.01$

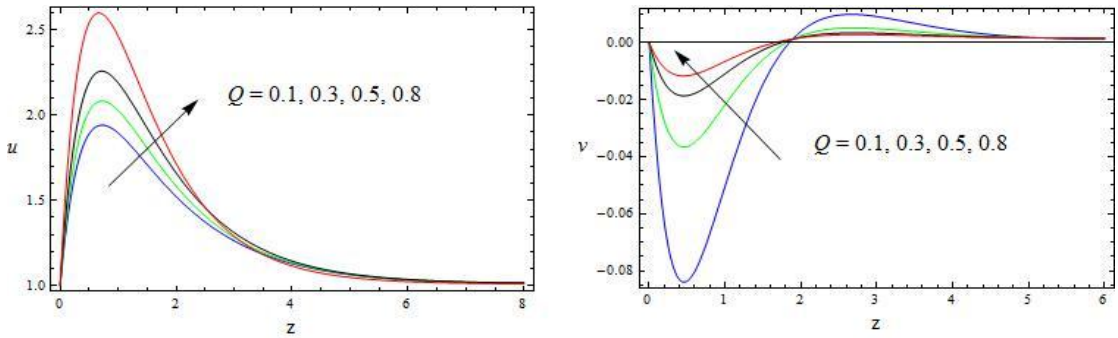

Figures 8. The velocity Profiles for u and v against Q

$M = 0.5, \varepsilon = 0.01, n = 0.5, A = 0.5, K = 0.5, \mathrm{Gr} = 3, \mathrm{Rm} = 0.01, \mathrm{Pr} = 0.71$

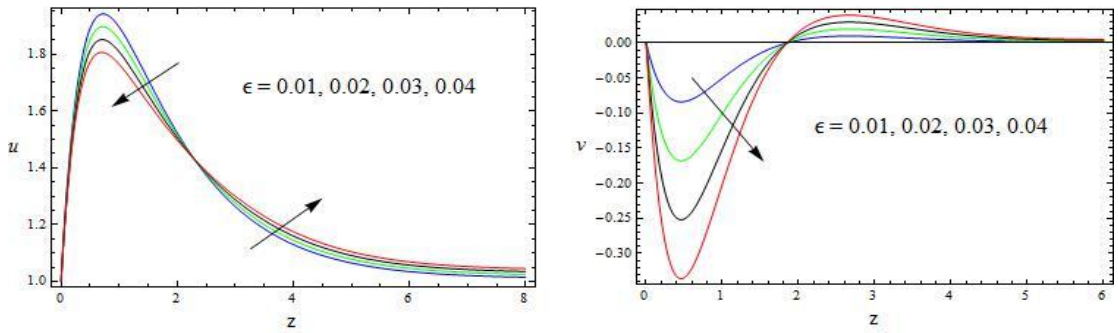

Figures 9. The velocity Profiles for u and v against ε

$M = 0.5, n = 0.5, A = 0.5, K = 0.5, \mathrm{Gr} = 3, Q = 0.1, \mathrm{Rm} = 0.01, \mathrm{Pr} = 0.71$

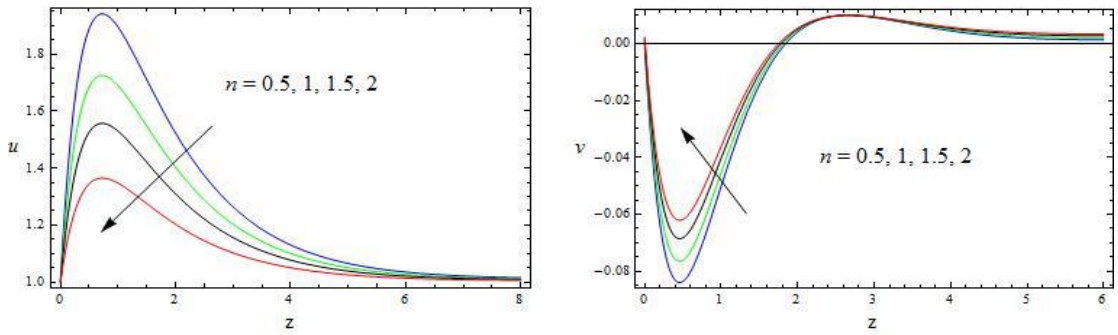

Figures 10. The velocity Profiles for u and v against n

$M = 0.5, \varepsilon = 0.01, A = 0.5, K = 0.5, \mathrm{Gr} = 3, Q = 0.1, \mathrm{Rm} = 0.01, \mathrm{Pr} = 0.71$

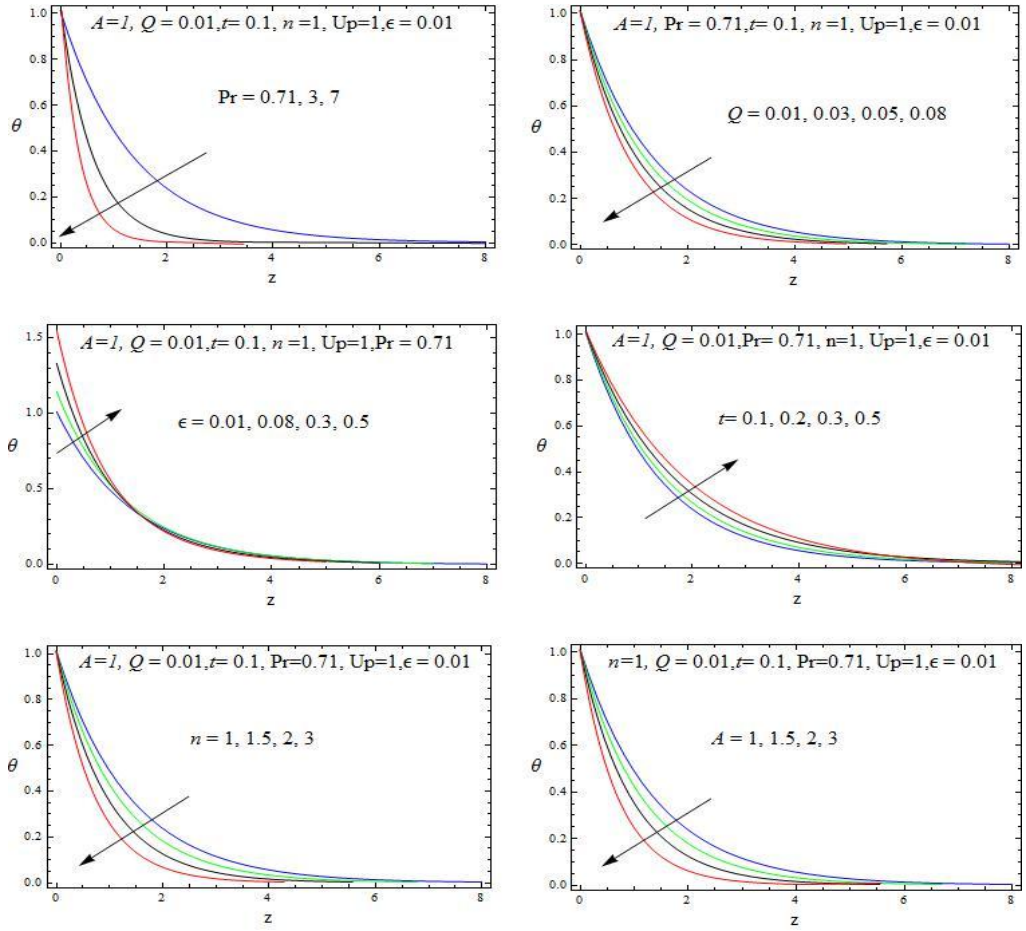

Figures 11. Temperature Profiles for θ against Pr, Q, ε , *t*, *n* and *A*

Table 1: Skin friction coefficient

M	***K***	**Gr**	**R_m**	***A***	**Pr**	***Q***	ε	***n***	τ_x	τ_y
0.5	**0.5**	**3**	**0.01**	**0.5**	**0.71**	**0.1**	**0.01**	**0.5**	3.85774	-0.038105
1									2.91287	-0.032129
2									2.09434	-0.023077
	1								5.17397	-0.035575
	1.5								7.16444	-0.011770
		4							5.13606	-0.051332
		5							6.41439	-0.064561
			0.03						3.82133	-0.038772
			0.05						3.78492	-0.039438
				1					3.81215	-0.013773
				1.5					3.76656	0.010559
					3				2.14603	0.049479
					7				0.64311	0.050748
						0.3			5.31207	-0.065335
						0.5			9.16266	-0.070009
							0.03		3.93626	-0.114315
							0.05		4.01478	-0.190525
								1	3.81864	-0.042519
								1.5	2.57448	-0.094433

Table 2: Nusselt number (Nu)

ε	A	Pr	Q	n	Nu
0.01	**0.5**	**0.71**	**0.01**	**0.5**	-0.733466
0.03					-0.760672
0.05					-0.787877
	1				-0.735992
	1.5				-0.738518
		3			-3.059900
		7			-7.123040
			0.03		-0.752536
			0.05		-0.770710
				1	-0.736135
				1.5	-0.738739

4. CONCLUSIONS

1. When scalar constant ε increase the velocity increase, whereas when dimensionless visco-elasticity parameter Rm and dimensionless heat absorption coefficient increase the velocity decreases.
2. Heat absorption coefficient Q increase results a decrease in temperature but, a reverse case is noticed in the presence of a constant ε.
3. It is recognized that there are many other methods that could be considered in order to describe some reasonable solution for this particular type of problem.
4. For better understanding of the thermal behavior of this work, however, it may be necessary to perform the experimental works.

APPENDIX:

$$m_1 = \frac{\mathrm{Pr} + \sqrt{\mathrm{Pr} + 4\mathrm{Pr}Q}}{2},\ m_2 = \frac{\text{-Pr} + \sqrt{\mathrm{Pr} + 4\mathrm{Pr}Q}}{2}$$

$$m_3 = \frac{\mathrm{Pr} + \sqrt{\mathrm{Pr}^2 + 4\mathrm{Pr}\left(Q+n\right)}}{2},\ m_4 = \frac{-\mathrm{Pr} + \sqrt{\mathrm{Pr}^2 + 4\mathrm{Pr}\left(Q+n\right)}}{2},\ N = M^2 + \frac{1}{K}$$

$$m_5 = \frac{-1+\sqrt{1+4N}}{2}, m_6 = \frac{1+\sqrt{1+4N}}{2},\ m_7 = \frac{-1+\sqrt{1+4N}}{2},$$

$$m_8 = \frac{1+\sqrt{1+4N}}{2},\ m_9 = \frac{-1+\sqrt{1+4\left(N+n\right)}}{2}$$

$$m_{10} = \frac{1+\sqrt{1+4\left(N+n\right)}}{2}, m_{11} = \frac{-1+\sqrt{1+4\left(N+n\right)}}{2}, m_{12} = \frac{1+\sqrt{1+4\left(N+n\right)}}{2}$$

$$a_1 = \frac{Am_1\mathrm{Pr}}{m_1^2 + m_1\mathrm{Pr} - \left(n\mathrm{Pr} + \mathrm{Pr}Q\right)},\ a_2 = 1 - a_1,\ a_3 = -\frac{\mathrm{Gr}}{m_1^2 - m_1 - N},\ a_4 = U_p - a_3 - 1$$

$$a_5 = -\frac{m_6^3 a_4}{m_6^2 - m_6 - N},\ a_6 = -\frac{m_1^3 a_3}{m_1^2 - m_1 - N},\ a_7 = -a_5 - a_6,\ a_8 = \frac{n}{N+n},$$

$$a_9 = -\frac{\mathrm{Gr}\,a_2}{m_3^2 - m_3 - \left(N+n\right)},\ a_{10} = -\frac{\mathrm{Gr}\,a_1}{m_1^2 - m_1 - \left(N+n\right)},$$

$$a_{11} = \frac{N}{N+n},\ a_{12} = \frac{Am_6 a_4}{m_6^2 - m_6 - \left(N+n\right)},\ a_{13} = -\frac{Am_1 a_3}{m_1^2 - m_1 - \left(N+n\right)}$$

$$a_{14} = a_8 + a_{11},\ a_{15} = a_{10} + a_{13},\ a_{16} = a_9 + a_{12} + a_{14} + a_{15}$$

$$a_{17} = Am_6^3 a_4 + Am_6 a_5 + m_6^3 a_{12} + nm_6^2 a_{12},\ a_{18} = Am_1^3 a_3 + Am_1 a_6 + m_1^3 a_{15} + nm_1^2 a_{15}$$

$$a_{19} = Am_8a_7,\ a_{20} = -m_{10}^3a_{16} - nm_{10}^2a_{16}$$

$$a_{21} = m_3^3a_9 + nm_3^2a_9,\ a_{22} = \frac{a_{17}}{m_6^2 - m_6 - (N+n)},\ a_{23} = \frac{a_{18}}{m_1^2 - m_1 - (N+n)}$$

$$a_{24} = \frac{a_{19}}{m_8^2 - m_8 - (N+n)},\ a_{25} = \frac{a_{20}}{m_{10}^2 - m_{10} - (N+n)},\ a_{26} = \frac{a_{21}}{m_3^2 - m_3 - (N+n)}$$

$$a_{27} = a_{22} + a_{23} + a_{24} + a_{25} + a_{26},\ a_{28} = -m_6a_4 - m_1a_3$$

$$a_{29} = -m_8a_7 - m_6a_5 - m_1a_6,\ a_{30} = a_{16}m_{10} - m_3a_9 - m_1a_{15} - m_6a_{12}$$

$$a_{31} = m_{12}a_{27} - m_6a_{22} - m_1a_{23} - m_8a_{24} - m_{10}a_{25} - m_3a_{26}$$

$$a_{32} = -m_1,\ a_{33} = -m_3a_2 - m_1a_1$$

REFERENCES

[1]. Kim, Unsteady MHD convective heat transfer past a semi-infinite vertical porous moving plate with variable suction. Int J Eng Sci 2000;38:833–45.

[2]. Chamkha Ali J. Unsteady MHD convective heat and mass transfer past a semi-infinite vertical permeable moving plate with heat absorption. Int J Eng Sci 2004;42:217–30.

[3]. Gokhale MY, Ali Samman FM. Effects of mass transfer on the transient free convection flow of a dissipative fluid along a semi infinite vertical plate with constant heat flux. Int J Heat Mass Transf 2003;46(6):999–1011.

[4]. Alam MS, Rahman MM, Samad MA. Numerucal study of the combined free forced convection and mass transfer flow past a vertical porous plate in a porous medium with heat generation and thermal diffusion. Nonlin Anal: Model Control 2006;11(4):331–43.

[5]. Hossain MA, Khanafer K, Vafai K. The effects of radiation of free convection flow of fluid with variable viscosity from a porous vertical plate. Int J Therm Sci 2001;40(2):115–24.

[6]. Seethamahalakshmi, Ramana Reddy GV, Prasad BDCN. Unsteady effects of thermal radiation on MHD free convection flow past a vertical porous plate. J. Comp. & Math.Sci. 2011;2(4):595–604.

[7]. Ahamed Sahin, Zueco J. Combined heat and mass transfer by mixed convection MHD flow along a porous plate with Chemical reaction in presence of heat source. Appl Math Mech 2010;31(10):1217–30.

[8]. Chaudhaury RC, Arpita J. Combined heat and mass transfer effects on MHD free convection flow past an oscillating plate embedded in porous medium. Rom J Phys 2007;52:505–24.

[9]. Ravikumar V, Raju MC, Raju GSS, Chamkha AJ. MHD double diffusive and chemical reactive flow through porous medium bounded by two vertical plates. Int J Energy Technol 2013;5(7):1–8.

[10]. Ravilumar V, Raju MC, Raju GSS. Heat and mass transfer effects on MHD flow of viscous fluid through non-homogeneous porous medium in presence of temperature dependent heat source. Int J Contemp Math Sci 2012;7:29–32.

[11]. Ravilumar V, Raju MC, Raju GSS. MHD three dimensional coquette flow past a porous plate with heat transfer. IOSR JMath 2012;1(3):03–9.

[12]. Singh KD, Kumar R. Fluctuating heat and mass transfer on unsteady MHD free convection flow of radiating and reacting fluid past a vertical porous plate in slip- flow regime. JAFM 2011;4(4):101–6.

[13]. Seethamahalakshmi, Prasad BDCN, Ramana Reddy GV. MHD free convective mass transfer flow past an infinite vertical porous plate with variable suction and soret effect. Asian J Curr Eng Maths 2012;1(2):49–55.

[14]. Rajesh V, Varma S Vijaya Kumar. Radiation and Mass transfer effects on MHD free convection flow past an exponentially accelerated vertical plates with variable temperature. ARPN J Eng Appl Sci 2009;4(6):20–6.

[15]. Israel-Cookey Ogulu A, Omubo-Pepple VB. Influence of viscous dissipation on unsteady MHD free convection flow past an infinite heated vertical plate in porous medium with time-dependent suction. Int J Heat Mass Transf 2003;46:2305–11.

[16]. Raju MC, Varma SVK. Unsteady MHD free convective oscillatory couette flow through a porous medium with periodic wall temperature. J Fut Eng Technol 2011;6(4):7–12.

[17]. Daleep K, Sharma, Ajaib S, Banyal. Bounds for complex growth rate in thermosolutal convection in Rivlin–Ericksen viscoelastic fluid in a porous medium. Int J Eng Sci Advan Technol 2012;2(6):1564–71.

[18]. Humera Noushima, Ramana Murthy MV, Reddy Chenna Krishna, Rafiuddin M, Ramu A, Rajender S. Hydromagnetics free convective Rivlin–Ericksen flow through a porous medium with variable permeability. Int J Comput Appl Math 2010;5(3):267–75.

[19]. Rana GC. Thermal instability of compressible Rivlin–Efficksen rotating fluid permeated with suspended dust particles in porous medium. Int J Appl Math Mech 2012;8(4):97–110.

[20]. Sharma RC, Sunil Suresh chand. Hall effects on thermal instability of Rivlin–Ericksen fluid. Indian J Pure Appl Math 2000;3(1):49–59.

[21]. Urvashi Gupta, Gauray Sharma. On Rivlin–Erickson elasticoviscous fluid heated and solution from below in the presence of compressibility, rotation and hall currents. J Appl Math Comput 2007;25(1–2):51–66.

[22]. Uwanta J, Hussaini A. Effects of mass transfer on hydro magnetic free convective Rivlin–Ericksen flow through a porous medium with time dependent suction. Int J Eng Sci 2012;1(4):21–30.

[23]. Varshney NK, Satyabhan Singh, Janamejay Singh. Effects of rotatory Rivlin-Ericksen fluid on MHD free convective and mass transfer flow through porous medium with constants heat and mass flux across moving plate. IOSR J Eng 2011;1(1):10–7.

[24]. Ravilumar V, Raju MC, Raju GSS, Varma SVK. Magnetic field effects on transient free convection flow through porous medium past an impulsively started vertical plate with fluctuating temperature and mass diffusion. Int J Math Arch 2013;4(6):198–206.

[25]. Seth GS, Ansari MdS, Nandkeolyar R. MHD natural convection flow with radiative heat transfer past an impulsively moving plat with ramped wall temperature. J Heat Mass Transf 2011;47(5):551–61.

[26]. Alam MS, Rahman MM, Sattar MA. Effects of variable suction and thermophoresis on steady MHD combined free-forced convective heat and mass transfer flow over a semi-infinite permeable inclined plat in the presence of thermal radiation. Int J Therm Sci 2008;47(6):758–65.

[27]. Rajasekhar K, Ramana Reddy GV, Prasad BDCN. Unsteady MHD free convective flow past a semi-infinite vertical porous plate. Int J Mod Eng Res 2012;2(5):3123–7.

[28]. Linga SC, Nazar R, Pop I. Steady mixed convective boundary layer flow over a vertical flat plate in a porous medium filled with water at 40 c: cases of variable wall temperature. Transp Porous Media 2007;69(3):359–72.

[29]. Muthucumaraswamy R, Ganesan P. Radiation effects on flow past an impulsively started infinite vertical plate with variable temperature. Int J Appl Mech Eng 2003;8(1):125–9.

[30]. K.V.S. Raju, T. Sudhakar Reddy, M.C. Raju, P.V. Satya Narayana, S. Venkataramana, MHD convective flow through porous medium in a horizontal channel with insulated and impermeable bottom wall in the presence of viscous dissipation and Joule heating. Ain Shams Eng J. 2014;5(2):543–51.

[31]. Satya Narayana PV, Venkateswarlu B, Venkataramana S. Effects of Hall current and radiation absorption on MHD micropolar fluid in a rotating system. Ain Shams Eng J 2013;4(4):843–54.

[32]. Mahgoub SE. Forced convection heat transfer over a flat plate in a porous medium. Ain Shams Eng J 2013;4(4):605–13.

[33]. Mukhopadhyay Swati. Slip effects on MHD boundary layer flow over an exponentially stretching sheet with suction/blowing and thermal radiation. Ain Shams Eng J 2013;4(3):485–91.

[34]. Sivaraj R, Rushi Kumar B. Chemically reacting dusty viscoelastic fluid flowin an irregular channel with convective boundary. Ain Shams Eng J 2013;4(1):93–101.

[35]. VeeraKrishna.M and B.V.Swarnalathamma (2016) Convective Heat and Mass Transfer on MHD Peristaltic Flow of Williamson Fluid with the Effect of Inclined Magnetic Field," AIP Conference Proceedings 1728:020461

doi: http://dx.doi.org/10.1063/1.4946512

[36]. Swarnalathamma. B. V. and M. Veera Krishna (2016) Peristaltic hemodynamic flow of couple stress fluid through a porous medium under the influence of magnetic field with slip effect AIP Conference Proceedings 1728:020603

doi: http://dx.doi.org/10.1063/1.4946654

[37]. VeeraKrishna.M and M.Gangadhar Reddy (2016) MHD free convective rotating flow of Visco-elastic fluid past an infinite vertical oscillating porous plate with chemical reaction IOP Conf. Series: Materials Science and Engineering 149:012217 doi: http://dx.doi.org/10.1088/1757-899X/149/1/012217.

[38]. VeeraKrishna/M and G.Subba Reddy (2016) Unsteady MHD convective flow of Second grade fluid through a porous medium in a Rotating parallel plate channel with temperature dependent source IOP Conf. Series: Materials Science and Engineering, 149:012216 doi**:** http://dx.doi.org/10.1088/1757-899X/149/1/012216.

[39]. Veera Krishna.M., B.V.Swarnalathamma and J. Prakash, "Heat and mass transfer on unsteady MHD Oscillatory flow of blood through porous arteriole, Applications of Fluid Dynamics, Lecture Notes in Mechanical Engineering, vol. XXII, pp. 207-224, 2018. Doi: 10.1007/978-981-10-5329-0_14.

[40]. Veera Krishna.M, G.Subba Reddy, A.J.Chamkha, "Hall effects on unsteady MHD oscillatory free convective flow of second grade fluid through porous

medium between two vertical plates," Physics of Fluids, vol. **30**, 023106 (2018); doi: 10.1063/1.5010863

[41]. Veera Krishna.M, A.J.Chamkha, Hall effects on unsteady MHD flow of second grade fluid through porous medium with ramped wall temperature and ramped surface concentration, Physics of Fluids **30**, 053101 (2018),

doi: https://doi.org/10.1063/1.5025542